Aus dem Department für Kleintiere und Pferde

der Veterinärmedizinischen Universität Wien

Institut/Klinik für Pferdechirurgie

Leiter: Univ.-Prof. Dr.med.vet. Florien Jenner Dipl.ACVS Dipl.ECVS

Comparing the difference in traction between the bare hoof, iron horseshoes and a glue-on model on different surfaces

Diplomarbeit

Veterinärmedizinische Universität Wien

vorgelegt von

Yuri Marie Zinkanel, 11828427

Wien, im Oktober 2022

1. **Betreuer:** Ao.Univ.-Prof. Dipl.-Ing. Dr.techn. Christian Peham
2. **Betreuer:** Dipl.-Ing. Dr.med.vet. Johannes Schramel

Eigenständigkeitserklärung

Hiermit erkläre ich, Yuri Marie Zinkanel, dass ich die vorliegende Arbeit selbstständig und nur mit Hilfe der angegebenen Literatur und Hilfsmittel verfasst habe. Alle wörtlichen und sinngemäßen Zitate wurden in der Arbeit als solche kenntlich gemacht. Alle relevanten Messungen wurden nach Anleitung des Betreuers selbst durchgeführt und protokolliert.

Weiters wurde diese Arbeit an keiner anderen Stelle publiziert oder veröffentlicht.

Wien, am 10.10.2022

Inhaltsverzeichnis

1. Introduction

1.1 Overview

Ever since the domestication of horses and the resulting increased workload put on the animals, especially their feet, on various surfaces that differ from their natural habitat of savannah and grasslands, humans have tasked themselves with the improvement of their health and safety, especially when relying on them for work and transportation. Forced to confront this problem, which in earlier times meant a lack of horses for armies and a decline of goods due to horses not fit for pulling carts, humans started devising the first types of hoof protection (Imhof, 2004).

In present times, the use for horses in the modernized world has shifted from a necessity for survival and warfare to uses in sport, either in a competitive or leisure setting. The demands for adequate hoof protection that is cheap, long living, practical in application and providing good interaction between the horses' legs and the ground have brought forth a great variety of options available on the market. While still used for its longevity, the traditional iron horseshoe is challenged by the rising options of glue-on models and hoof shoes when it comes to surface interaction and practicality while also able to provide better cushioning of the hoof on hard ground (Cheramie & O'Grady, 2003).

The various ground surfaces that the horse has to maneuver on in its daily life in a regular stable facility make a strong grip a necessity. Previous studies suggest a direct correlation between the amount of sliding on ground and resulting injuries, which often affect the tendons of the lower limb (Peterson et al., 2012). From the indoor concrete floors to the loading and parking area's asphalt coatings, the various competition grounds made of sand, mud, grass and, depending on the season, also ice challenge the traditional shoeing methods and paved the way for alternatives that are better suited for ground conditions and the horses' health while working.

Regarding the impact on performance, the force applied onto the limb in order to propel the horse forward when moving through competition courses has to be adjusted by the horse and stands in direct correlation to the grip provided when interacting with the ground, having to adjust the applied force and the directly related speed to avoid slipping, hindering the horse during the competition (Tan & Wilson, 2011).

Taking this into consideration, the aim of this paper is to compare the different rotational resistance (representing the grip) of the bare hoof, traditional iron shoes and a glue-on model on various surfaces in order to determine the strengths and weaknesses of each tested application.

1.2 Hypothesis

Previous studies analyzed the results of variable grip in different shoeing options and on various grounds indirectly, for example through the displacement of jockeys' center of mass during gallop (Horan et al., 2021). This paper aims to directly measure the rotational resistance representing the grip of three common conditions of the hoof, being either the bare hoof, shoed normally or having a glue-on model applied. The results are given in absolute numerical data and as combinations between the surfaces and the applications respectively.

The testing was conducted without relying on living horses. Instead, the Vienna Grip Tester was used in order to achieve a continuous controlled testing environment and set up in order to produce results that are not influenced by individual horses' anatomy and conformity regarding stride length or weight. This leads to an easier comparison and less disturbance of the measuring caused by outside variables.

Hypothesis: The glue-on horseshoes provide a higher grip on all surfaces than the traditional horseshoe and the bare hoof.

2. Literature Overview

2.1 Anatomical overview of the lower limb

When referring to the distal part of the horses' extremities, the skeletal components involved are the distal phalanx bone, also known as coffin or pedal bone in most literature, the distal sesamoid bone, which is often referred to as the navicular bone and the distal part of the second phalanx bone. These bones interact with each other through their various articular surfaces. To provide a complete clinical overview, the Latin nomenclature of the following structures has also been added in cursive, taken directly from the Illustrated Veterinary Anatomical Nomenclature (Schaller, 2007). The distal phalanx mainly interacts with the second phalanx through its *caput phalangis mediae*, forming the distal interphalangeal joint. The second and third articulation involves the distal sesamoid bone, which has two surfaces involved to firstly form a joint with the distal phalanx and, further proximal, one which interacts with the middle phalanx. Furthermore, various ligaments and cartilages add support and stability to the lower limb.

In order to provide a sufficient overview of the structures that make up the lower limb, including the hooves, this part of the paper will provide an anatomical overview of the aforementioned structures.

There are three main surfaces on the distal phalanx bone. The first one is the porous dorsal wall (facies parietalis), which is in direct contact with the capsule of the hoof through neurovascular structures. The second surface, *facies solearis*, is partly in contact with the sole of the hoof through its *planum cutaneum*, with the other part (*facies flexoria*) serving as the flexor surface for the attached tendons and ligaments. The *linea semilunaris* is the structure that devides these two surfaces. The articular surface, located at the upper part of the bone, differs from the ones found on the other phalanx due to it being divided into two areas. The flatter region of this surface accommodates the navicular bones while the other interacts with the middle phalanx.

The *margo coronalis*, the proximal border of the distal phalanx, extends at the dorsal midline as a processus for the common or long digital extensor tendon. The complimentary border of the most distal part of the bone, where the *facies solearis* and the parietal surface meet is called the *margo solearis*. The *processus palmaris medialis* and *lateralis* serve as a palmar extension on the bone, with each having their own foramen (*foramen processus palmaris*

medialis and *lateralis*) or notches (*incisura processus palmaris medialis* and *lateralis*) to provide a pathway for blood.

Additionally, various groves and foramina allow for a sufficient blood supply. The most notable ones are the *foramen soleare mediale* and *laterale*, which allow the passing of the digital arteries into the solear canal. Furthermore, sulci, which are defined as grooves in the bone, act as a gateway for the digital arteries in order to reach the aforementioned foramina. Grooves on the parietal wall (*sulcus parietalis medialis* and *lateralis*) connect the process foramen or notches of the palmar *processi* towards the dorsal midline of the bone.

Various cartilages, tendons and ligaments are involved in the joints' structures. The palmar or plantar side of the distal sesamoid bone is also called the flexor surface since the deep digital flexor tendon (DDFT) passes over it, aided by the navicular bursa (*bursa podotrochlearis*) in order to glide unhindered and protected from the bone. The DDFT connects to the collateral cartilages (*cartilage ungularis medialis* and *lateralis*), which are located at the palmar or *processi* of the distant phalanx along the semilunar line of the bone. They also provide a pathway for the vascular system to the venous plexuses.

The collateral ligaments (*Ligg. Collateralia med.* and *lat.*), which run on the medial and lateral side of the distal interdigital joint, provide stability on both sides. The collateral sesamoidean ligaments (*Ligg. Sesamoidea collateralia*), which are also known as suspensory ligaments connect the distal sesamoid bone to the second phalanx. The distal border of the sesamoid bone is connected to the flexor surface of the distal phalax through the distal sesamoidean impar ligament (*Lig. Sesamoideam distale impar*), also known as DSIL. It inserts palmar to the DDFT, resulting in a densely packed collagen bundle and provides room for the neurovascular system and elastic fibres.

The ungual cartilages are attached to the bone or each other through five ligaments. The cartilage is connected to the prox. phalanx through the *Ligg. chondrocompedalia*, to the middle phalanx through the *Ligg. chondrocoronalia*, to the palmar process of the dist. phalanx with the *Ligg. chondroungularia collateralia* running straight and the *Ligg. chondorungularia cruciate* crossing over to the other side respectively. The *Ligg. chondrosesamoidea* connects the cartilage to the distal sesamoid bone.

Considering this anatomic blueprint, the previously mentioned joints connecting the phalanges are hinge joints, also occasionally classed as saddle joints because of their ability to also rotate and bend laterally and medially to a small degree. The distal interphalangeal joint also permits

a great degree of movement on the area articulating with the second phalanx. The articulation towards the navicular bones however is a rather fixed construct with very little to no movement in the joint.

Considering that the lower parts of the horse's limb is devoid of muscles and only reached by the tendons in their stead, extra protection of these more fragile structures is essential. On the dorsal side of the distal interphalangeal joint the *recessus dorsalis* reaches proximally along the second phalanx bone to situate itself between the bone and the common digital extensor tendon. Similarly, on the palmar side of the joint the *recessus palmaris* is located right at the palmar surface of the middle phalanx, separated into two parts, one located cranially and one caudally.

The navicular bursa acts as a cushion between the distal sesamoid bone's flexor surface and the DDFT, further reaching into the lower part of the limb to separate the *Lig. sesamoideum distale impar* and the lower part of the DDFT (Parks, 2003).

2.2 The hoof capsule's epidermis

The hoof itself has different organic tissue and various areas. The subcutaneous tissue, the dermis and the epidermis provide the basic structure of the capsule and layer on top of each other. The outer most layer, the epidermis, is comprised of hard keratin, which originates from the basal layer (*stratum basale*) on the coronary segment of the hoof. The *stratum germinativum* is made up of the aforementioned *stratum basale* and additionally the *stratum spinosum*, into which the cells that were produced in the basal layer migrate into. This segment of the hoof accounts for almost all of the horn produced (McKittrick et al., 2012).

Similar to the anatomy of the bones, the hoof capsule also has designated names for its areas. The hoof horn in toto is called the *capsula ungulae*. The outside dermis that makes up the wall is called *paries corneus* and divides into three parts, the lateral outer part, the medial inner part and the dorsal or toe part, located between the previously mentioned ones. The heel of the hoof, located at the caudal area of the hoof is also named after its position on the hoof, dividing into a lateral (*pars mobilis lateralis*) and a medial part (*pars mobilis medialis*). The caudal part of the horn turns back up to the coronary border both lateral and medial, forming the bars (*pars inflexa lateralis* and *medialis*).

Similar to the underlying bone structure of the distal phalanx, the proximal border of the hoof is called *margo coronalis* and the distal part that comes into contact with the ground is called

the *margo solearis*. The last border structure runs from the palmar caudal angle of the heel towards the coronary border and is known as the *margo palmaris lateralis* and *medialis*.

The layers of the hoof wall are the outer *stratum externum*, the *stratum medium* and the *stratum internum*. The perioplic segment, which resides under the coronary band area of the hoof, is the origin of the external layer and extends proximally as the so-called coronary band, which consists of unpigmented and soft intertubular and tubular horn and distal as a more hardened, water-resistant glossing on top of the actual horn wall. To summarize, the outer layer acts as a protection film to keep the hoof save from environmental influences such as water that could lead to deterioration of the horn.

Underneath this glossy outer layer is the mass-bearing middle layer, which originates from aforementioned *germinal epithelium* and continues its growth as long as the animal is alive (Daradka & Pollitt, n.d.). It provides an additional average 6 to 8 mm of horn growth per month, which can be influenced by vibration caused by movement of the limbs in various gates (Halsberghe, 2018). The microscopic make up of the horn, which shows a tubular arrangement of the alpha-keratin that originated from the keratinocytes, is primed by the existence of the coronary dermal papillae (*papillae dermales*). The keratin tubes reach from their growth zone all the way to the ground and have a diameter of 0.2 mm and comprise the tubular section of the horn tissue. In between those structures lays the intertubular horn, which stems from the space around the coronary dermal papillae and can either be pigmented or not on the outside and middle layer of its section (Schummer & Nickel, 1981). The way these tubulars are oriented in angle and density help with distributing strain and lessen the probability of breakage of horn in this layer. The innermost part of the intertubular horn is not pigmented and joins the middle layer of the horn to the innermost layer.

While providing stability through its special tissue blueprint of surrounding keratinocytes with a protein matrix and crosslinking with intramolecular and intermolecular bridges, the wall's rigidness lessens the further it reaches into the inner parts of the horn, which allows for force-absorption in this specific area. This provides optimal transfer of the load from movement to the adjoined inner layer of the dermis. The ability to bind moisture into the horn furthermore enforces a more elastic behavior, which allows the hoof to deform to a certain degree. The open-ended hollow tubes that have ground contact on the other hand allow moisture to leave the horn. (Kasapi & Gosline, n.d.)

The *stratum internum*, which is in direct contact with the dermis of the hoof, is made up off primary epidermal lamellae (*lamellae epidermalis*) and secondary epidermal lamellae. The primary ones originate from the proximal lamellar growth zone, which lays at the inner part of the coronary segment and travel to the palmar contact zone of the horn. The secondary lamellae are responsible for the connection of the epidermis with the dermis and are derived from the primary lamellae. In order to do so, these secondary lamellae are, contrary to the primary ones, not as hard since there are less keratinized structures involved. Instead, they are formed by a middle longitudinal axis that is coated with basal cells. Furthermore, their shapes are different, as the primary lamellae are rectangular, allowing for a firm fit against each other and a big surface area. The secondary ones are rounded on one end and fit against a basement membrane, which round over the tips of the secondary lamellae in a snug fit, bordering onto the dermis (Pollitt, 2004).

This leaves the epidermal part of the sole, which is similar to the epidermis on the wall of the hoof. In general, the sole is made up of the main middle part, the *corpus solae*, and the side parts medially and laterally (*crus soleae medialis* and *lateralis*). The horn for these regions comes from the sole epidermis (*epidermis soleae*) and makes up the largest part of the solear capsule surface. The sole connects to the wall part of the hoof through the *margo parietalis*, which runs parallel to the inside wall. Here, the while line, or *linea alba* is formed by the connection of these areas. The connection to the frog, which is framed by the two sole legs, is made through the *margo centralis*. The horn on the sole also consists of horn tubules, which grow towards the ground into the sole epidermis, influencing the sole's thickness and leading to a significantly firmer outer part near the hoof wall and a thinner part around the apex of the frog.

The hoof pad (*torus ungulae*) is divided into a base and an apex, the former being located furthest palmar in between the bar of the hoof, with the apex, also known as frog (*cuneus ungulae*), reaching towards the middle of the sole and also dorsally into the sole. The horn of the frog is derived from the germinal epithelium of this region (*epidermis cunei*). It shares the same property of horn as the previously mentioned wall, having tubular horn surrounded by intertubular horn. The groves that frame the frog (*sulcus paracunealis medialis* and *lateralis*) on the sole develop from the frog's medial and lateral crus, which are located between the apex and the pad, and are divided into their respective parts by the central groove (*sulcus cunealis centralis*). This same grove can be projected internally into the frog and is known as the *spina cunei*, or the spine of the frog. The heel bulbs (*torus corneus, pars medialis* and

lateralis) are a continuation of the frog further palmar and wrap towards the hoof wall, finishing the capsules outer layer (Schummer & Nickel, 1981)

2.3 The hoof's dermis (corium)

When looking at the anatomical blueprint of the dermis, it quickly becomes obvious that it shares the most important features with the epidermis of the hoof. The horn production of the tubular horn once again stems from the perioptic part (*dermis limbi*), which intersects with the perioplic groove of the outer proximal hoof wall. The perioplic dermis' path widens towards the heel bulbs and connects to them. The horn tubules are derived from the dermal papillae. The coronary band is formed by the coronary dermis (*dermis coronae*) slotted into the coronary groove of the epidermis, the germinal epithelium responsible for cell production, and the subcutaneous tissue furthest in. The area of the coronary dermis proximally is called the perioplic dermis, reaching distally and continuing as the parietal dermis (*dermis parietis*) or the wall part. It makes its way towards the corium part of the frog's crura on the sole while interacting with the lateral parts of the wall's horn.

The horn tubules, similar to the horn of the epidermis layer, stem from the coronary dermal papillae. The ridged surface of these papillae allows for more areas of contact between them and the germinal zone while also guiding the tubules of horn on their way down during their growth. Consistent with the middle wall of the epidermis horn, this area of horn also experiences lower density further into the hoof (Pollitt, 2004)

When leaving the coronary zone of the dermis, the parietal zone continues, made up of dermal lamellae (*lamellae dermales*) that are sectioned into primary and secondary parts (Pollitt, 1996)

Contrary to the epidermal primary lamellae, which are formed like clubs, the secondary dermal lamellae taper towards their tips in order to connect to the epidermal basal cells of the primary epidermal lamellae. Both dermal and epidermal lamellae come together to anchor the inner hoof wall with the outer dorsal surface of the hoof. This process stops when the solear surface is reached by the horn and is substituted by a plug of terminal papillae that insert themselves into the space left by the absence of the dermal lamellae.

After reaching the solear area of the hoof, the border between the sole and the parietal wall is efficiently sealed by tubular and intertubular horn that originates from the germinal epithelium that fills the gaps in the epidermal lamellae. This tissue has contact with the ground and, because of its lack of pigment, appears pale yellow leading to the name white line of the hoof

(*linea alba unglae*). Wrapping over towards the sole, the dermis adheres to the solear surface of the hoof bone as the *dermis soleae*, also anchoring itself into the epidermis of the sole, the frog and the heel through papillae. Furthermore, the dermis of the sole and the frog (*dermis cunei*) connect, which also leads to a connection to the dermis of the heel bulb (*dermis tori*) (Pollitt, 2010)

2.4 The hypodermis

There are various areas of hypodermic tissue spread throughout the areas of the hoof underneath the dermis, acting as a shock absorbing cushion made of collagen, adipose tissue, blood vessels, nerves, cartilage and elastic fibers. The most proximal one is called the perioplic tissue (*pulvinus limbi*), which is continued by the coronary cushion (*pulvinus coronae*) derived from the subcutaneous tissue (*tela subcutanea coronae*) of the coronary area. This particular area also leads to the convex curvature of the dermis in this region.

While a potential parietal and sole part of the hypodemis is not described consistently throughout literature, the digital cushion (*pulvinus digitalis*) located at the pad of the hoof formed by the *tela subcuntanea tori* spans over the bulb of the heel (*pars torica pulvini digitalis*) towards the frog dermis (*pars cunealis pulvini digitalis*), dividing it into the two respective parts. This specific area is also crucial for allowing better blood flow through the lower limb through its vascular structure (Bowker & Linder, n.d.).

2.5 Vascular system in the hoof

The blood supply of the equine distal extremity is made up of many, sometimes merging, arteries and veins. Considering the make up of the lower leg and all its joints and tissues, the division of the blood vessels into different zones is a sensical conclusion. These zones can either be independent or interacting with each other. Generally, the two interacting zones run along the dorsal part of the leg as the primary proximal and secondary distal zone. The third zone supplies the palmar part of the extremity independently (Parks, 2003). Beginning the dorsal interacting zones with the main digital arteries, the *Aa. Digitales medialis* and *lateralis* and their venous counterparts travel along the sides of the leg, entering the solar canal after passing through the solear groove and the solear foramen, uniting into the terminal anastomose in the canal, the so calles *arcus terminalis*.

Before passing the most proximal interphalangeal joint, the *ramus tori digitalis* splits of from the arteries in order to supply the palmar structures, like the frog’s dermis, the regions

responsible for horn growth, the heels and bars, the deep digital flexor tendon, the hoof cartilages, the distal sesamoid bone and the distal interphalangeal joint and the *bursa podotrochlearis*.

Another split-off occurs either from the main artery or the *ramus tori digitalis* respectively in form of the *A. coronalis*. This vessel continues to run along the dorsal contour of the ungual cartilage and the horn capsule. The last part of the two dorsal zones consists of the *ramus dorsalis phalangis mediae*, which is derived from the digital artery at the level of the second phalanx, continuing its path distally over the dorso-axial side of the cartilage in order to anastomose with the vein. The coronary and perioplic horn growth segment, the upper part of the wall segment, the extensor tendon and the joint connecting the second and third phalanx receive their oxygen supply through these vessels. The complimenting branch on the palmar side, the *ramus palmaris phalangis mediae* completes the surrounding of the medial phalanx.

The *ramus dorsalis phalangis distalis* originates from the previously mentioned main digital arteries on the dorsal side when passing distal sesamoid bones respectively, making their way along the distal phalanx' palmar process and the following parietal groove. As indicated by their pathway along the outside of the bone, these vessels provide the blood flow along the parietal wall segments of the palmar heel and the quarters, uniting with the *A. marginis solearis* on the named after its location on the solear border.

The previously mentioned *ramus dorsalis* of the distal phalanx continues distally to enter the porous parietal wall of the bone to supply the distal dorsal zone together with the *arcus terminalis* (Schummer & Nickel, 1981).This arc's branches travel through the solear canal and its many small openings to distribute themselves through the entire bone. While the parietal wall is passed by these small vessels to merge with the branches of the coronary segment, there is also a anastomose further distal with the *A. marginis solearis*, which is primarily responsible for the supplementation of the sole, aided by the parietal branches that join this vessel to palmary pass the solear border

Taking this into account, the consequences of the uneven distribution of the vessels and the resulting lack of blood supply in certain regions of the distal phalanx, namely the lack of blood flow through the mid parts of the solear surface and the bone processi belonging to the extensor tendon, are a decreased chance of fracture healing directly correlated with the amount of perforation in the area. On the other hand, the well supplied border of the sole has

a far better chance of healing due to its generous supply from the *A. marginis solearis* (Schade, S. M., Arnoczky, S. P., & Bowker, R. M, 2014).

As per usual, the large arteries are accompanied by their venous counterparts, like the *V. digitalis medialis* and *lateralis*, with the coronary vein, the caudal hoof vein of the digital pad, the terminal arcus and the vein along the solear border receiving sufficient drainage from various plexi in order to sufficiently cycle through the oxygen (Mishra & Leach, 1983). These plexi are names after their location on the hoof, with the coronary plexus situated at the coronary cussion in the segment, reaching over to the abaxial area of the hoof cartilage. Similarly, the dorsal plexus resides in the dorsal region of the hoof, specifically in the lamellar dermis of the wall segment. Lastly, the palmar plexus, as per its name, drains the sole in the solear dermis and makes its way further proximal on the axial surface of the cartilage, fusing with the coronary plexus in an anastomose while passing through the cartilage in the hoof (Pollitt, 2004)

As mentioned previously, the anatomy of the of the distal phalanx bone with its many big and small foramina is crucial to supply the dermis sitting on top of the bone, which in turn is essential to keep the basal cells of the lamellae working and the hoof growing.

The frequency of motion and in turn loading and unloading of the supporting limb adds to the amount of perforation the hoof experiences, in turn impacting the health of the whole hoof organ (Medina-Torres et al., 2016).

2.6 Nerves of the distal limb

The digital nerves running along the medial and lateral sides of the lower limb, the *N. digitalis palmaris (proprius) medialis* and *lateralis*, are responsible for the innervation of the hoof. They supply the outer parietal hoof wall, the solear surface, the frog and the heels, while additionally reaching deeper into the tissue of the distal extremity. The structures affected further in the limb are the joints, with all their bones and cartilages, the tendons and ligaments situated in this distal area. When reaching the upper sesamoid bones, the nerves branch of dorsally into the *ramus dorsalis*, leading to the perioplic and coronary growth segment of the hoof after passing over the dorsal and lateral surfaces. The solear canal's blood vessels are also accompanied by this branch, passing through it to towards the wall segment, providing a solid network for vibrational, pain and nociceptic input (Schumacher et al., 2013).

2.7 Basics of friction

In order to bridge a possible knowledge gap, a brief introduction in the basic principles of friction is included in this work. Friction is created by the interaction of an object's surface with another surface. This interaction is strongly influenced by surface types, ranging from rather smooth like ice to rough surfaces, like concrete and gravel. This leads to a restriction of the object to move from its position on another one's surface, resulting in standstill of the object or, under the influence of a directional force, movement against the factor of friction. While this phenomenon also occurs in gasses and liquids, the main focus in this paper lies in the interaction of solid objects, in this specific case the hoof and all applications and the test grounds.

Generally speaking, three types of friction exist. The most basic one is referred to as static friction responsible for holding an object in place even if the surface it is placed on is tilted to a certain degree. When taking a microscopic look at the surfaces, an uneven pattern can be observed on close to all surfaces. These individual groves interact with each other, hooking into the other surface, which creates the effect of static friction. After reaching a threshold the static friction is not sufficient enough to hold the object in place. This limit marks the maximum static friction force between the object and the corresponding surface it is placed on. In the testing method used in this study, no tilting of the surfaces was used, ensuring that the tested application were always placed at a 90 degree angle on the ground.

While the influence of the tilt does not influence the static friction in this case, the mass of object and in our case the mass applied through the Vienna Grip Tester has a directly proportional influence, which is why the direct number can be put into the equation to quantify the grip force. In this case, the same amount of force was applied through the system during all measurements. The variable factor in our case was the surface quality of the application and the ground. This in general is hard to quantify and usually is factored in through premeasured materials. This variable differs from application to application and most surface types can be looked up in preexisting tables.

In order to measure a static friction force, an antagonizing force has to be added. This works against the static friction. By adding more force towards the object, the static friction force also heightens proportionally until the threshold is reached. This allows for an approximation of static friction force by relying on the amount of force applied until the object moves.

Once this happens, sliding friction occurs. It leads to a decrease in the force that holds the object in place. During the movement, the sliding friction works against the force that put the object into motion. Similar to the static friction force, this force is also tested out between various surface types and put into tables for easier use (Roth & Stahl, 2016).

While not relevant to this study, another type of friction, the one occurring while an object is moving over a surface in a rolling pattern, can be observed. It is based on the weight of the object deforming the object itself and the surface it passes over, leading to a sinking into the surface due to the mass. The deformation of the surface manifests in a small, raised section on the surface cause by the weight of the object, which has to be passed in order to proceed with the rolling motion. This type of friction is also dependent on the material surface qualities and further on the radius of the object (Roth & Stahl, 2016).

3. Materials and Methods

3.1 Materials

For this project, seven different surfaces that are relevant for performance in sport and the safety of the horse in its daily living environment were tested, including concrete and asphalt in dry and wet state, grass, sand and ice. These tests were conducted for three different types of hoof protection (traditional iron shoes and two pairs of glue-on shoes, the second one functioning as a reference of a model without additional grip plates, provided by N&U Sport Horse Shoes GmbH) and the bare hoof without any additional protection.

The surfaces as well as the natural hoof and its applied protection are assigned corresponding letter combinations as ID. The following tables 1 and 2 include every tested surface and hoof application.

ID	Surface	Description
BT	concrete dry	VetMed Track for checking soundness
BN	concrete wet	VetMed Track for checking soundness
AT	asphalt dry	VetMed Track for checking soundness
AN	asphalt wet	VetMed Track for checking soundness
GR	gras	Garden of the VetMed University
SD	sand	VetMed Track for checking soundness
E	ice	Artificial ice block, 20 cm diameter

Table 1: abbreviations of the different surfaces used in the test

ID	Hoof application	Description
BH	natural bare hoof	A natural bare hoof provided by the anatomy department of the VetMed Vienna
BK	plastic glue-on shoe	Provided by the N&U Sport Horse Shoes GmbH
GK	anti-slip glue-on shoe	Provided by the N&U Sport Horse Shoes GmbH, fitted with additional anti-slip plates

E	iron horse shoe	A commercial iron horse shoe fitted on a metal plate, provided by the VetMed Vienna

Table 2: abbreviations of the different test models

Preparations for measuring

The measurements of the rotational grip on the different surfaces were conducted on the facility of the University of Veterinary Medicine Vienna (VetMed Vienna). The different tracks to determine lameness in horses outside of the university's riding arena were used as test grounds. Before the testing all used materials and surfaces were assigned and ID and fitted onto the Vienna Grip Tester. In order to conduct the testing an additional person was needed to properly use the equipment and who also put the results of the measurements in a handwritten protocol, which was later digitalized and is attached as a table.

Data collection and analysis

The data was collected through the use of a torque wrench (DTW-100f, Checkline Europe, Germany) fitted onto the Vienna Grip Tester (Fig. 1) provided by the Movement Science Group of the VetMed University Vienna (Peham & Schramel, 2017). The maximum torque (rotational resistance) on every surface was measured in Nm. A total of 20 measurements with a load of approximately 700 N were taken per ground and hoof protection combination, resulting in 560 measurements which were later digitalized (see appendix chapter). The spring used in this Grip Tester is the Monroe "Heckklappendämpfer" (ML5653), which has an extension force of 550 N on its own, with the added weight of the whole apparatus the whole force amounts to approximately 650 to 700 N of force. The measurements were imported into the program SPSS to evaluate and compare the different measurements taken from different hoof samples on the same ground with each other. In order to compare the different surfaces and hoof applications the average, the minimum and the maximum results including outliers were taken into consideration

3.2 Methods

Test Procedure

The fitting of the different hoof protection was done in the treadmill hall (room PE05A00) of the VetMed University Vienna by the author. In order to mount the natural bare hoof onto the application, a metal joint comprised of a plate on the upper part of the hoof and a metal rod that could be fitted into it were used. The same mechanism was also used on the iron horseshoe, ensuring that the hoof application was sitting plane on the tested surface. The glue-on variants were fixed onto the iron plate with metal screws instead of the usual attachment onto the hoof with glue. This made for easier changing of the application and prevented wear on the natural bare hoof's walls. In order to conduct measurements on ice an artificial block of ice had to made in the freezer of the anatomy department of the university, which was transported to the test location (Fig. 2).

Figure 1: testing conducted on sand with the Vienna Grip Tester: the device is lowered on the ground, with the hoof application sitting flat on the surface. The person conducting the test and an assistant step into the steel stir-ups with their right foot, pressing them towards the ground to make contact with it. This assures that the applied force has the correct load of 700N on the gas spring, which is encompassed into the metal tube used as casing. The wrench shown in the right picture is then twisted 45 ° in order to take the measurement. The number on the display shows the grip measure in Nm.

Before starting the tests, the surfaces were inspected in order to avoid using a faulty surface (for example dirtied or wet). The surfaces were tested in the same order for every hoof variable to achieve reliable results that were not influenced by the application being worn down on previous surfaces. In order to use the Vienna Grip Tester two people step into the stir ups, applying a force of 700 N onto the tested surface-hoof combination through a spring (Fig. 1). This compresses the spring in the device in order to apply the load onto the hoof extension. The wrench is twisted by 45 degrees by the person conducting the test and the result is copied down from the display of the torque wrench. The wrench measures the height of static friction achieved by the tested application on each surface due to the usage of the maximum hold function, measuring the amount of applied force it takes for the hoof application to turn on the surface. After each measurement, the testing equipment and the attached hoof variant are lifted off the surface completely in order to assure that the next measurement isn't compromised by the previous one. A video demonstration of the testing device can be found on YouTube (Vetmeduni, 2015). The measurement on the ice were conducted last and on a different day to prevent the block from melting and thus providing compromised results (Fig. 3).

In this study, a torque wrench with a maximum hold function has been used to identify the static friction of the application-surface combination. The torque is a vector momentum which is calculated by the radius of the wrench arm and the force applied to this arm in order to move the object, or in this case the force that has to be applied to lead to a rotation on the surface. The formula for this is $M = r * F$, with M being the torque, r the radius and F the force (Brommundt et al., 2007).

This can be modified by including the factors of spinning friction which modifies the formula as follows: $Ms = f * N * rm$, with Ms being the rotational friction, N the variable for the normal pressure and rm the average radius of the contact point between the interacting surfaces, in our case the ground and the hoof application. The coefficient of the spinning friction, $\mu s = f * rm$, has to be experimentally determined (Hamel, 1912).

After each different surface, the used hoof variant was cleaned with a brush to get rid of excess material stuck on it, which could influence the subsequent tests on a different surface. Additionally, the location on the softer surfaces was switched every two measurements in order to get accurate results, as the grass and sand was giving in under the pressure.

Additional measurements were taken on asphalt and cement, after spraying it with water in order to simulate realistic everyday circumstances after rain or in facilities where water is used regularly like washing facilities and the like.

Figure 2: track for testing soundness of the horse on the campus of the university

Figure 3: artificial ice block used for testing with a diameter of 25 cm

Hoof variants

Four types of hooves were used for this test series, a natural hoof provided by the Department of Anatomy without any additional protection (Fig. 4), a traditional iron horseshoe and two glue-on variants provided by the N&U Sport Horse Shoes GmbH (Fig. 5). While conducting the measurements, the hoof and shoes were placed flat onto the tested surface and the Grip Tester was held in a 90 degree angle. The glue-on variants were applied to the iron shoe application instead of the bare hoof to allow for easier fitting and removal. This does not influence their grip when conducting these measurements.

Figure 4: natural hoof

Figure 5: glue-on shoe with grip-plates

Each mentioned variant was tested 20 times on all surfaces to allow for more accurate interpretation of the measurements through a broader sample size. Furthermore, due to their nature, the tested surfaces exhibited deviation from a plane surface, resulting in tilting of the device if not noticed beforehand. Even though the unevenness of the surface would be expected in a non-scientific, daily use when training and working with horses, special care was taken in order to get accurate results on the grip by choosing even spots on the track and retaking measurements if outside parameters, like gravel or sand on asphalt track was noticed. The data was used in order to compare the hoof applications on all surfaces and subsequently rank them based on their grip. The p-value was taken into consideration to interpret the significant or insignificant differences between the various hoof models.

Statistics

The software SPSS (27.0, IBM Chicago, Illinois, USA) was used to compare the differences. Normal distribution of the data was checked with the Kolmogorov-Smirnov-Test. To compare the different groups (surfaces and hoof shoes) an ANOVA for repeated measures was used. The Bonferroni correction was used to avoid the multiple comparisons problem. The results of the tests were put into Microsoft EXCEL and later imported into SPSS for processing. The boxplots used were also made with SPSS, the tables displaying the data were taken from the statistics output of SPSS.

4. Results

4.1 Comparison of surfaces and hoof applications

When comparing the different surfaces with each other, there was a significant difference in grip when testing the artificial building surfaces, dry and wet concrete, dry and wet asphalt, with p= 0.00, while grass showed a significantly higher grip than sand (p= 0.00), ice (p=0.00) and dry asphalt (p=0.02). Sand on the other hand provided significantly less rotational grip compared to all other surfaces (p=0.00) besides ice (p=0.17).

The highest measurement for traditional iron horseshoes were taken on grass, with an average of 16.5 Nm ± 0.87 compared to the lowest one, which was taken on ice and amounted to 6.5 Nm ± 0.36, both showing a significance of p=0,01. The glue-on grip variant provided a much better grip on all tested surfaces, also excelling on grass with a grip almost as high as the one provided by the natural bare hoof in raw measurement data, with p=1.00 showing an insignificant difference. The grip measured on the ice averaged 12.8 Nm ± 1.26 which is a significant improvement compared to the second highest grip provided by the bare hoof, measuring 10.23 Nm ± 0.76 and amounting to a difference of 2.57 Nm, with p=0.33. The natural hoof provided the second-best grip on ice, but the worst on sand.

The traditional iron horseshoe provided significantly less grip regarding the average than all other applications, with significance varying between p= 0.000 and p= 0.004. The special grip plate model showed a significant difference in grip only when compared to the traditional iron shoe with p= 0.00.

Tables containing the average and the standard deviation of all measurements are included in the appendix of this paper (table 3-6).

4.2 Comparing the different surfaces

The following comparison shows the difference in rotational grip of different surfaces, in order to visualize the amount of grip expected and to be able to rank them from highest to lowest rotational grip. When tested, the surfaces showed a wide spectrum of grip when looking at the average from all tested hoof applications, with surfaces associated with stable grounds, like asphalt, cement and grass consistently having a higher grip value than the sand that is used in riding arenas. The weather specific surface of ice and the used sand have only little difference in their overall ability to provide grip paired with all tested hoof applications.

When the average rotational grip of each surface is considered, grass is shown to have the highest grip out of all tested surfaces, closely followed by dry concrete. Sand and ice provided the worst grip, amounting to a difference of 13.03 Nm between grass and sand.

The boxplot (Fig. 6) below shows the difference in Nm regarding the rotational grip of all hoof applications on the grass surface. Notably, only the artificial bare hoof (BKGR) shows no distinct outliers. The traditional iron horseshoe (EGR) and the natural bare hoof (BHGR) have minima outliers, the most extreme being a grip of 5 Nm from the combination of iron shoes and grass as a surface. The special glue-on grip variant has one maximum outlier. The difference in grip between the iron shoe and all other applications is significant with a p=0.00 for all, between each other they all showed a p > 0.05.

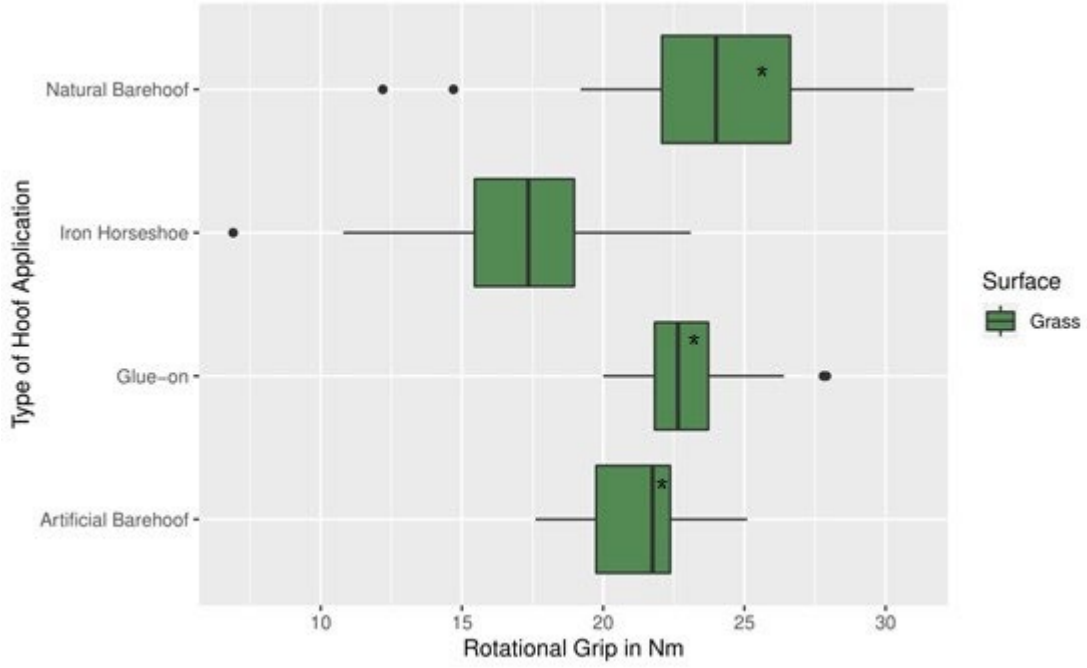

*Figure 6: comparison of rotational grip of all hoof applications on grass, additionally showcasing a significant difference in grip through the asterisk * symbol when compared to the iron shoe. The boxes show the range from the first to the third quartile and include 50% of all data. The circles show the outliers, which present themselves outside of the whiskers that are normed by 1.5 times the interquartile range.*

Both glue-on models show a wide range in grip on dry asphalt (GKAT & BKAT), the model without the grip plates providing significantly stronger grip on dry asphalt (22.41 Nm ± 1.24 for

BKAT and 20.35 ± 1.11 for GKAT) with p=0.00 for both compared to the iron shoe , and the one with grip plates taking the lead on wet asphalt (23.55 ± 1.06 for GKAN and 19.31 Nm ± 0.83 for BKAN) while showing a significantly higher grip regarding p=0.00 and p=0.01 in when compared to the iron shoe and the artificial bare hoof respectively.

The natural hoof provides a strong grip considering the average grip of all applications, on dry (BHAT) and wet (BHAN) asphalt, surpassing the average grip of the iron shoes on the surface significantly with p=0.00 for both, while also having a wide distribution of grip strength. When comparing average data of all applications they closely follow after both glue-on models (Fig. 7).

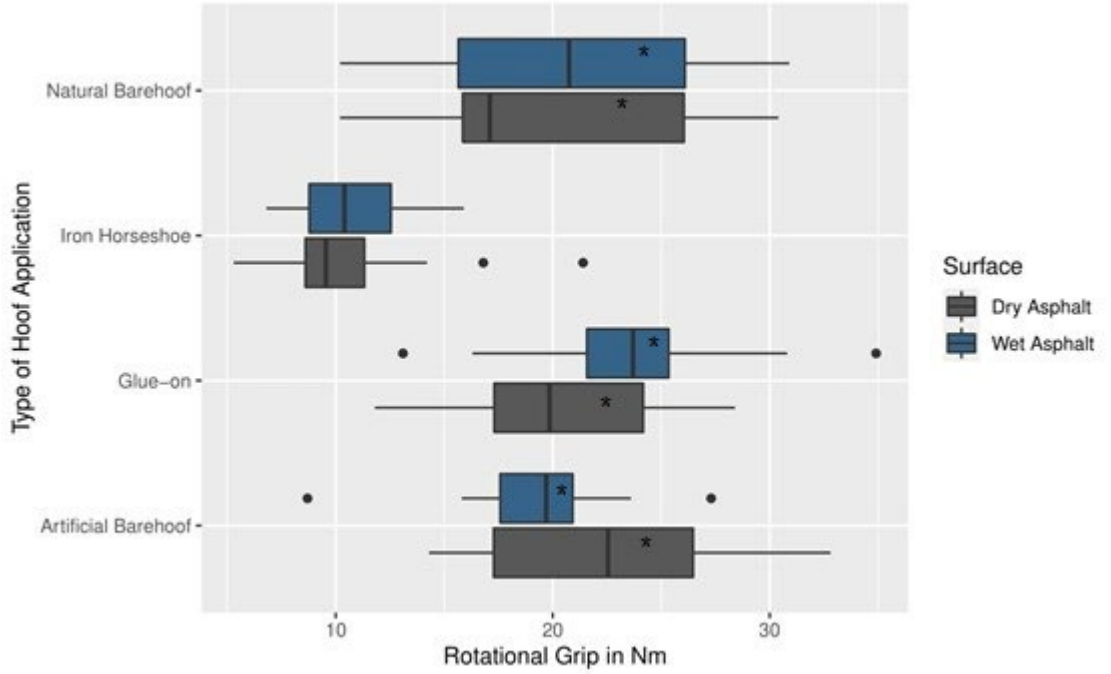

*Figure 7: comparison of rotational grip of all hoof applications on dry and wet asphalt, additionally showcasing a significant difference in grip through the asterisk * symbol when compared to the iron shoe. The boxes show the range from the first to the third quartile and include 50% of all data. The circles show the outliers, which present themselves outside of the whiskers that are normed by 1.5 times the interquartile range.*

Considering the boxplot below, it is easily noted that an icy surface proves to be a challenge for all the tested hoof applications, with iron horseshoes faring the worst out of all and showing very little range in grip. There extreme outliers are located above the upper whisker, showing

some instances where the grip was rivaling the one of the natural bare hoof. The second and third quartile have little variation in grip compared to the other models.

The special glue-on grip model, having a wide range of grip strength, provided the best grip on the ice while also showing a significant difference in grip compared to the iron shoes with p=0.00 and also to the artificial bare hoof with p=0.01. The median 50% of data are located significantly higher when compared to the other models, with the fourth quartile showing a considerable range of measurements.

The natural bare hoof locates itself between the previously mentioned applications, providing a relatively well distributed grip range without any extreme outliers, followed by the plastic bare hoof model used for comparison with the one fitted with grip plates (Fig.8).

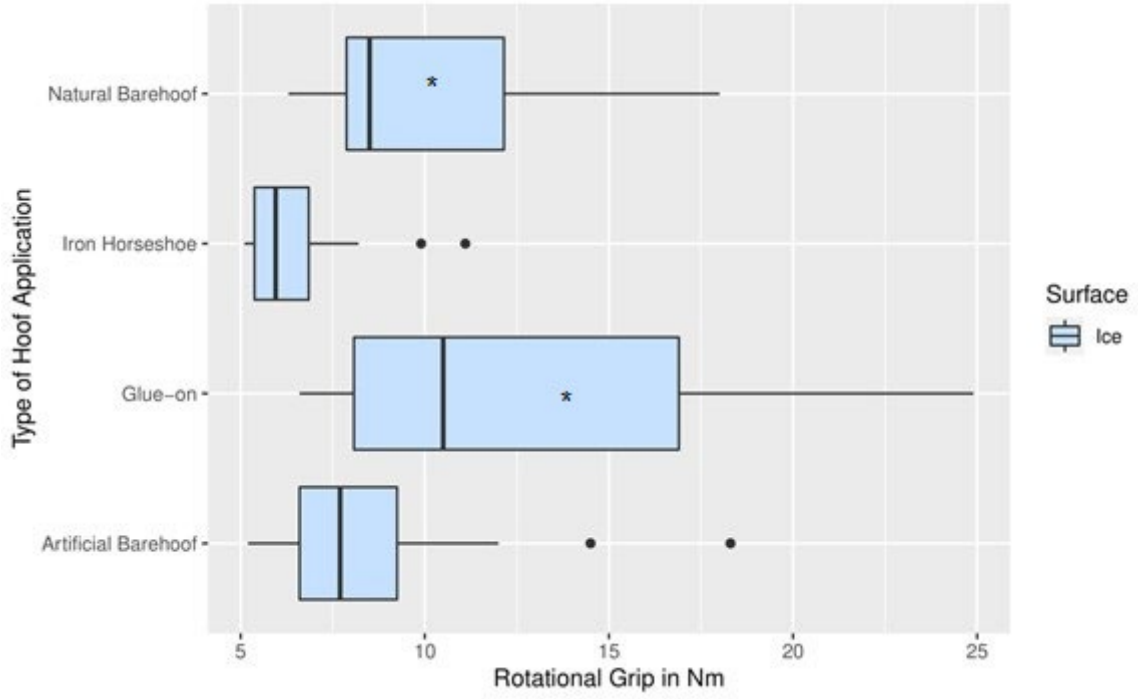

*Figure 8: comparison of rotational grip of all hoof applications on ice, additionally showcasing a significant difference in grip through the asterisk * symbol when compared to the iron shoe. The boxes show the range from the first to the third quartile and include 50% of all data. The circles show the outliers, which present themselves outside of the whiskers that are normed by 1.5 times the interquartile range.*

With sand being the one surface most horses are trained and competed on, the choice of the hoof application is crucial for performance. The measurements show that, while not being the best option, the traditional iron horseshoes (ESD) provide decent grip with a wide range of grip strength, amounting to an average of 7.78 Nm ± 0.24. When compared to the bare hoof (BHSD), the difference in grip was statistically insignificant with a p=0.09, which had the lowest grip strength and little variation in grip, measuring 6.86 Nm ± 0.19. The special grip glue-on shoes (GKSD) and the one without the grip plates (BKSD), originally used for comparison in order to determine the usefulness of the plates, settled at first and second place respectively with both showing a significant increase in grip strength compared to the bare hoof (p=0.00 and p=0.01 respectively). Their boxes and whiskers show relatively similar data in all four quartiles without any outliers. When comparing the average grip data of the two on this surface, the grip of the model with special plates amounts to 8.93 Nm ± 0.35, while the comparison model shows data at 8.9 Nm. Considering this, the difference in grip between those two models is miniscule on the sandy surface with a p=1.00 (Fig. 9).

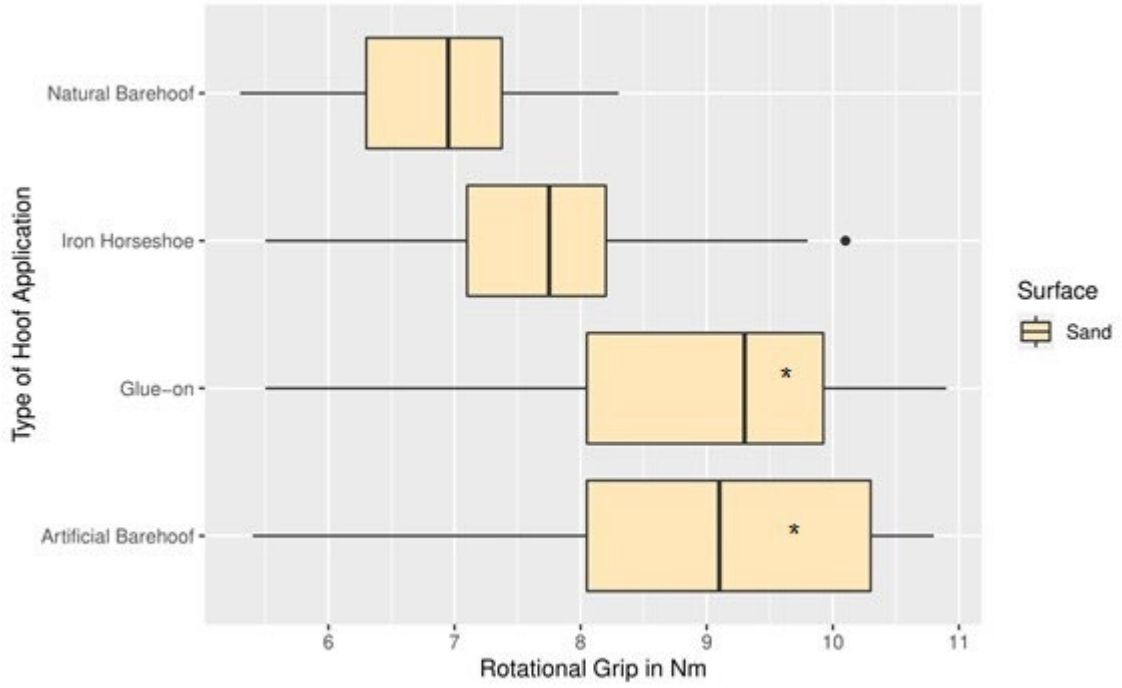

*Figure 9: comparison of rotational grip of all hoof applications on sand, additionally showcasing a significant difference in grip through the asterisk * symbol when compared to the natural bare hoof. The boxes show the range from the first to the third quartile and include 50% of all data. The circles show the outliers, which present themselves outside of the whiskers that are normed by 1.5 times the interquartile range.*

4.3 Comparing the different hoof applications

The following section shows a comparison of one application each on all tested surfaces. This visualizes the strengths and weaknesses of all tested hoof variants.

The first diagram (Fig.10) displays the data of the iron horseshoe. The grip on wet and dry concrete is similar, averaging at 13.91 Nm ± 1.1 and 14.55 Nm ± 1.16 respectively. Asphalt provides a visibly worse grip in both states, averaging at 10.50 Nm ± 0.84 on dry and 10.64 Nm ± 0.53 on wet grounds. The best overall grip of the iron shoe was provided by grass, with an average of 16.46 Nm ± 0.87. The tests on sand and ice showed a relatively low grip of 7.78 Nm ± 0.24 and 6.50 Nm ± 0.36, leaving it as the worst application on both surfaces combined, with only the bare hoof gripping worse on sand

The plot also shows the various outliers. The minimum outliers in the gras data also show that the iron shoes grip on the surface is rather unreliable sometimes, even though the overall grip seems to be quite high compared to other surfaces. The maximum outliers on the other surfaces do not significantly better the grip strength and would rather be viewed as coincidental in this case.

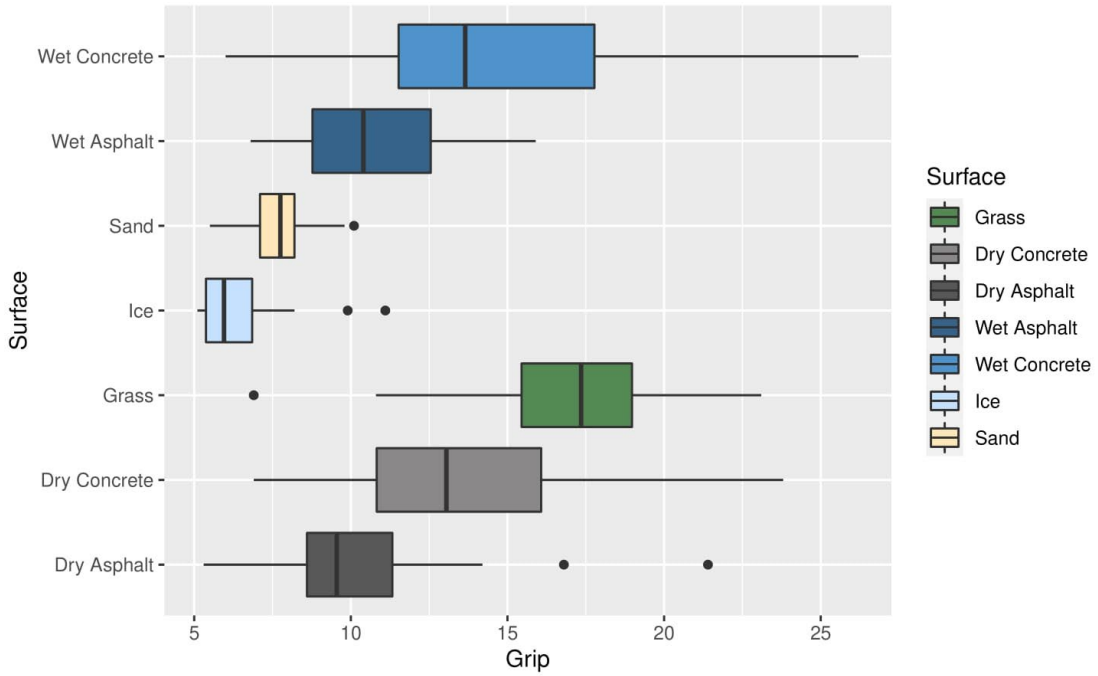

Figure 10: comparison of rotational grip of traditional iron shoes on all tested surfaces

The special grip model shows a relatively well distributed grip quality on all surfaces, excluding sand and ice, with only one minimum outlier measured on wet asphalt, which simultaneously also provided the best overall average grip of 23.55 Nm ± 1.06 (Fig. 11). In comparison, this hoof application showed a relatively small grip spectrum with maxima outliers on grass, resulting in a short box and small whiskers in the diagram and an overall well grip that is only surpassed marginally by the natural hoof when competing on the grass as a surface (p=1.00). The measured average grip for this combination shows a grip of 23.16 Nm ± 0.47.

On dry concrete, the glue-on grip model performed almost as well as the natural hoof (22.17 Nm ± 1.02 compared to 22.60 Nm ± 1.90, p=1.00 showing an insignificant difference) and surpasses it in performance on wet concrete with a difference of 4.07 Nm (p=0.10). Dry asphalt provided the least grip out of all stable surfaces with an average of 20.35 Nm ± 1.11.

Compared to all other tested applications, this grip model excelled when tested on sand and ice. Between this model and the artificial bare hoof, a significant difference of 4.27±0.41 Nm and a p=0.01 in grip was measured on the ice surface, amounting to 12.80 Nm ± 1.3 with the grip plate model and 8.54 ± 0.74 with the artificial bare hoof respectively.

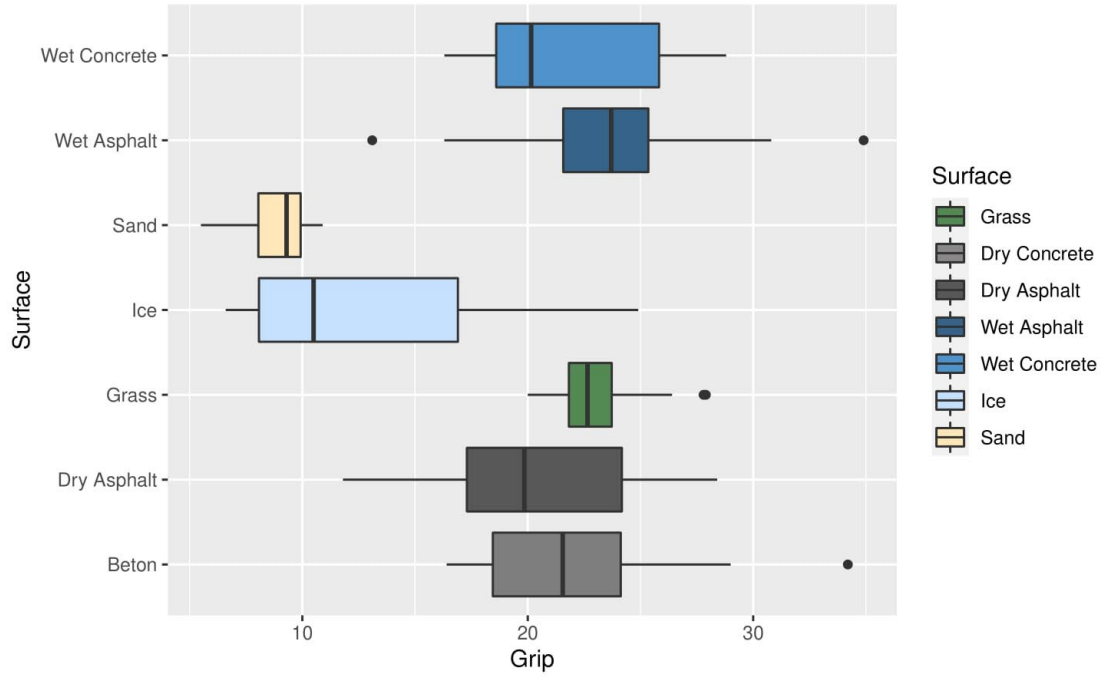

Figure 11: comparison of rotational grip of glue-on model with grip plates on all tested surfaces

The bare hoof without additional shoeing allowed for an overall good grip, except for sand and ice. Out of all tested applications, this one showed the worst grip on sand with an average of

6.86 Nm ± 0.19, with grip as low as 5.30 Nm and the highest taken measurement amounting to 8.30 Nm, providing a significantly worse grip then the grip plate application (p=0.00) and the srtificial bare hoof (p=0.01). When tested on ice, the grip measured was significantly higher than the iron horseshoe with a difference of 3.73 Nm (p=0.00) and an average grip of 10.23 Nm ± 0.76 when using the natural hoof application and 6.50 Nm ± 0.36. On all facility surfaces a wide range of grip was observed, but no maximum or minimum outliers were found, resulting in a reliable grip (Fig. 12). The combination of the natural hoof with the grass surface yielded the best results out of all tested applications, providing an average grip of 23.60 Nm ± 1.00. A few minima outliers can be seen outside of this box, indicating that, although the grip is strong, it is probable for it to fare worse on the surface from time to time.

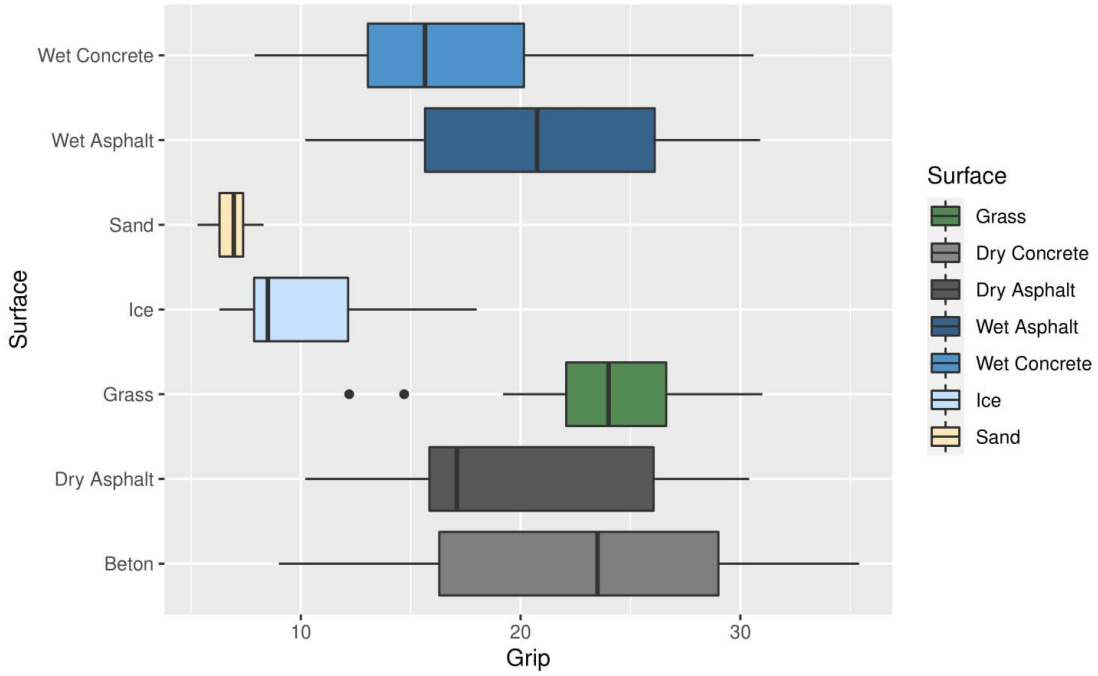

Figure 12: comparison of rotational grip of the natural hoof on all tested surfaces

5. Discussion

The hypothesis that the glue-on model provides a better grip on all surfaces than the bare hoof and the traditional iron shoes has been partially verified through this study, with the results showing a significantly better grip on all surfaces besides grass, where the grip model was surpassed by the natural bare hoof, and sand where the hoof shoe model without the grip plates scored higher, followed closely by the grip plate model.

The digital organ of the horse in all its complexity has to be taken into consideration when looking for the right fit of hoof protection, whether it is to be used in competitive sport or leisurely. The complicated biomechanical blueprint of the horse's lower limb is not made for most of today's surfaces, since the living environment of these animals changed drastically from the wild roaming horses. This results in inadequate grip and heightened wear on the digital organ and the following joints of the limb. While some heightened resistance of the ground can be beneficial to the horn growth due to stimulation of vibration (Halsberghe, 2018), too much movement on rigid surfaces can cause wear on the other parts of the biomechanical system, like the joints. The suspensory apparatus of the distal limb in the capsule is a rather delicate and intricate system which relies heavily on the overall health of the horse.

Over the years a lot of different variations of iron shoes have appeared on the market to be modified by the farrier in order to meet the needs of different horses with various hoof conditions, such as laminitis or white line disease. While providing a fair selection, the make up of such iron shoes may not be beneficial for all horse and rider combinations. Some horses, be it either because of their training and living environments or a required flexibility in shoeing, need a different approach in order to bring out the best in their performance and health, especially when they are trained, ridden or pulling carriages on harder grounds. While iron shoes allow only for movement of the heel and keep the rest of the hoof static, the new shoeing options allow for more motion in the whole hoof due to the difference in material and fixation. Often times, these applications also include the heel, reducing the frequent problem of heel wear that causes a flatter angle of the dorsal wall over time (Parks, 2003).

Recently, various forms of hoof shoes and glue-on models have shown to be effective, especially on slippery surfaces like ice and wet concrete. While hoof shoes offer a rather limited time of protection, usually only worn while the horse is being exercised and are to be taken off after riding, a glue-on model is a more permanent and practical solution that is applied to the hoof after a trim and kept on until the next trim. The fixation through gluing it directly onto the

hoof wall is durable enough to withstand the horses' need for movement inside its stable, the paddock, field or on the training grounds. Horses with hoof conditions, such as broken out walls that require a rather short trim especially benefit from this application because of the extra protection of the sensitive thin sole and short walls. This prevents further lameness through cushioning the hoof against hard grounds and gravel, lifting the sole further from the ground and often providing a closed plate on the bottom. This prevents bruising on the sole when trimmed too short or from it not being concave enough. Additionally, fixation on the outer wall rather than through nailing into the horn can prevent further breakage in the sensitive regions and prevent nailing injuries on the sole, which would also result in lameness that shows right after the application of the iron shoes and, depending on the length of the nails used and the specific placement, can take months to fully grow out. This problem occurs more often with the commercially premade iron shoes, since they do not provide adequate angles on the nailing site, resulting in injuries on the white line or the horn (O'Grady & Poupard, 2003).

The results of this study show a promising amount of rotational grip on various surfaces when the glue-on model was used. Unsurprisingly, the grip plates incorporated into this model excelled on usually difficult to navigate surfaces, like ice and grass whereas the traditional iron shoe struggles to provide a sufficient grip. This especially makes it a viable option for riders that compete and ride in cross-country setting in various types of weather, providing a safety when navigating difficult terrain through forests, fields and occasional icy patches on the ground. While the bare natural hoof provides sufficient grip on most of these surfaces as well, though still subpar compared to the glue-on model, the amount of work that causes wear on the horn without protection could potentially be detrimental to the overall health and soundness of the horse.

Furthermore, the grip of the plates used in the model also holds up much better on asphalt and concrete, whether it be wet or dry, providing a higher degree of safety while riding or leading the horse on streets or stable grounds than the bare hoof, potentially lowering the risk of sliding while navigating the surface through riding or during loading and unloading of the horse into the trailer. This could be a measure of prevention regarding the horse's own health, avoiding potential muscle and ligament tear on one hand, while also decreasing the chance of collateral damage on property or the people handling the horses.

The iron shoes on the contrary lack the imitation of the natural, rather flexible and slip resistant sole and wall that the glue-on model imitates, providing the worst grip on concrete and asphalt

surfaces. While it outperforms the natural hoof on sand of riding arenas, it is surpassed by the tested grip plate model on this surface as well. The iron variant also provides the least amount of grip on ice.

When comparing the model with the grip plates with the second one provided by the company that lacks these, the interactions with the ground can be put into perspective. Unsurprisingly, the surface of the application without grip plates lies flatter on the ground, which resulted in more grip on concrete, be it wet or dry, and dry asphalt. On the contrary, the wet asphalt made for far better interaction with the plates than without, providing better stability on the slippery and smooth ground. The same can be said for grass and the underlying ground soil where the plates could sink better into the, comparatively, softer surface.

While sand proved itself to be a rather challenging surface for all applications, both of the provided plastic models had better ground interaction than all other applications, with the grip plate model taking the lead. On ice, the same results could be observed during the test, with the un-plated model falling behind the natural hoof and the plated model taking the lead.

Taking these results into account, the choice of using a glue-on model with grip plates is favorable over traditional shoeing in all accounts when comparing the rotational grip, while it still may be falling behind the natural hoof horn on grass during the testing. The difference between these two subjects can be classed as minimal regarding the data.

The focus of this study has been solely on the grip strength and was carried out through a set testing system by a measuring tool (Vienna Grip Tester) and not on live horses in order to provide a controlled measurement environment. The set-up allowed the measurements to be taken at the same angle, force and degree of rotation each time. While quite practical for a material study, this also means that certain areas like fitting, comfort for the horse, impact on the gait and durability have not been taken into account when ranking the applications. Furthermore, only the standard u-shaped iron shoes were tested during this study, ignoring the various other form options on the market, that while less common, could potentially provide a better grip than the standard shape. Additionally, neither hoof studs nor snow grips were applied on the iron shoe, which are widely available options often in use in colder regions or during the winter to prevent slipping without having to rely on specific models of hoof protection that may not be as widely available.

Additionally, the used hoof applications varied in height, with the natural bare hoof adding the most height to the test set up. The height difference between the various application causes a

slight difference in the pressure applied when testing the models. As a result, this height would have to be taken in consideration when comparing the different measurements. Because the spring used is a gas spring, the general characteristic curve that shows the influence of displacement in height on the produced force is relatively shallow, which means that the influence of additional height could be overlooked in this case. However, no characteristic curve was available for the specific gas spring model used in this study. If this same spring is to be used in further studies, the characteristic curve should be measured beforehand in order to get the raw grip measurement without the falsification due to application height, be it a significant difference or not.

Further studies conducted when the horse is in motion, favorably on a treadmill set-up with capture through slow motion cameras could provide further insight into the impact of the shoeing on the gait while walking, trotting and cantering. The gait of each individual horse is slightly different, varying in the area of footing on the hoof, be it rather plane or with the cranial or caudal area of the hoof first. The concept of dynamic balance of the hoof has to be taken into account no matter which hoof protection is chosen, since establishing a geometrically and dynamically balanced hoof should be the end goal of all shoeing methods. This ensures that the hoof anatomy is near to symmetrical when divided through the middle axis and the footing is as plane as the horse's gait conformation allows. This leads to proper distribution of the force on the solar border (O'Grady & Poupard, 2003).

These variations of anatomy and gait can influence the durability and application, since different forces on the gluing points have to be considered. The durability of these new models would have to be checked after the wearing period to see if the models could be reapplied or if a new set of shoes are needed. Another important factor that must be considered is the health of the outer hoof wall that comes into contact with the glue. Generally, there are four base materials used as adhesives, namely polymethyl methacrylate acrylics (PMMA), cyanoacrylates, polyurethanes and epoxies. All except the cyanoacrylates are commercially available as a two-part mixture, while the former is already premixed in the container or tube. Cyanoacrylates, widely known as superglue, has a comparatively shorter curing time than the other variants, however its use is limited to the treatment of smaller cracks and defects, since a too thick application can hinder a thorough bonding process. This problem does not occur in the other mentioned adhesives.

While this study puts importance on the horse's shoeing to provide a stable hoof-ground interaction, the measurements taken are the sum of the grip between the actual layer that touches the hoof and the underlying materials. The way riding surfaces are built try to ensure a top layer that allows for sufficient slide when the horse touches down in its gait to absorb the impact shock and a manageable amount of grip between the particles in order to allow for the surface to move under the hoof. The middle layer ensures stability and further shock absorption (Swedish Equestrian Federation's reference group for riding surfaces, 2014).

Previous studies show the importance of surface layer mixtures and the amount of moisture in the layer to influence the grip. Linke (2016) and Semmelrock (2017) both incorporated the measuring of the moisture in the top layer of the surface and the resulting influence on the grip provided during surface interaction. This factor has not been included in the conducted measurements during this study.

While being less taxing on the horse due to the avoidance of smoke and loud noise during application, the curing process generally emits heat during the process, which could result in aversive reactions of the horse. None of the mentioned glue formulas result in health complications during and after the shoeing if the proper application process is followed thoroughly (Cheramie & O'Grady, 2003).

Additionally, depending on the location, not many farriers may yet offer the service of applying these shoes to horses because of their usual focus on steel shoes that are still widely used in horse sports. While this issue could be alleviated by the further spread of new hoof applications, the fact that not much testing has been conducted yet may affect the initial reluctance to make use of the new shoeing methods on the market. Offering a thorough manual to farriers and other professional personnel and additional courses on the benefits of glue-on shoes could serve as a breakthrough point on the market as well, allowing for development of further improved models.

After having an in-depth look into the anatomy, it is clear that the health of the hoof relies on a lot of factors, which includes the protection of the horn. The literature used is comprised of various publications from different authors which were mostly sourced through the search engine PubMed and ScienceDirect. Above all, the professional opinion of farriers and veterinarians should be taken into consideration before changing the current shoeing on a horse. With the recent advancements of shoeing options, a change of hoof protections on

horses with different needs will surely occur more often than ever before, with the riders and their horses reaping the benefits of the new models.

6. Summary

Zinkanel Yuri Marie (2022)

Comparing the difference in traction between the bare hoof, iron horseshoes and a glue-on model on different surfaces

The aim of this test series was to provide a comparison of grip strength provided by different hoof applications consisting of commercially available iron shoes, the bare hoof, a plastic bare hoof model and a special anti-slip plate model on the most common surfaces of horse facilities. The testing was conducted manually with the Vienna Grip Tester by taking 20 measurements on each application-to-surface combination.

The models tested as follows between the highest and lowest measured grip across all surfaces: traditional iron horseshoe from 5.1 Nm to 26.2 Nm, natural bare hoof from 5.3 Nm to 35.4 Nm, the grip-plate model from 5.5 Nm to 34.9 Nm and the artificial bare hoof from 5.2 Nm to 33.4 Nm. The average grip and the standard deviation of each surface and hoof application were calculated in order to compare the taken measurements.

This test series showed that there is a clear advantage in grip when using the special grip plate model compared to the iron horseshoe on and in most cases the natural bare hoof. The durability and the influence of change of the surface quality of the application during wear has not been tested, since this was a study conducted without animal testing and, considering the average shoeing period of most horses, would not have been possible. The hypothesis, that glue-on horseshoes provide a higher grip on all surfaces than the traditional horseshoe and the bare hoof has been partially accepted.

In the future, more material components should be evaluated to be used in horse’s hoof protection to find the optimal fit for a guaranteed grip increase through the application, preferably also incorporating the quantity of shock absorption and durability during the active wear period.

7. Zusammenfassung

Zinkanel Yuri Marie (2022)

Gripvergleich zwischen Naturhuf, Hufeisen und einem Hufschuhmodell mit Grip-Platten auf verschiedenen Untergründen

Das Ziel dieser Arbeit war es, die unterschiedlichen Grip-Stärken eines traditionellen Hufeisens, des Naturhufs, eines künstlichen Naturhufs und eines Hufschuhmodells mit speziellen Grip-Platten auf verschiedenen, im Stall üblichen, Untergründen zu messen und diese miteinander zu vergleichen. Die Testreihe wurde mit Hilfe des Vienna Grip Testers durchgeführt und es wurden 20 Messungen pro Beschlag-Untergrund Kombination ausgeführt.

Die verschiedenen Modelle zeigten folgenden minimalen und maximalen Grip auf allen getesteten Böden: das Hufeisen zwischen 5,1 Nm und 26,2 Nm, der Naturhuf zwischen 5,3 Nm und 35,4 Nm, das Grip-Platten Modell zwischen 5,5 Nm und 34,9 Nm und der künstliche Naturhuf zwischen 5,2 Nm und 33,4 Nm. Aus diesen Daten wurden die Mittelwerte und Standardabweichungen jeder Hufapplikation und Boden Kombination errechnet, um diese zu vergleichen.

Den gemessenen Größen kann ein deutlicher Unterschied im Grip entnommen werden. Das spezielle Hufschuhmodell schneidet auf den meisten Untergründen als bester aller Beschläge ab und übertrifft somit das traditionelle Eisen und meistens auch den Naturhuf. Die Abnützung der Beschläge und deren Einfluss auf den Grip wurden in dieser Versuchsreihe nicht getestet, da keine Lebendtierversuche mit durchschnittlichem Beschlagzyklus durchgeführt wurden. Die Hypothese, dass das glue-on Model auf allen Untergründen besseren Grip als traditionelle Hufeisen und der Naturhuf zeigt wurde teilweise angenommen.

In Zukunft könnten mehr Materialien auf ihre Qualität und Einsetzbarkeit für den Hufbeschlag getestet werden, die einen noch besseren Grip, eine bessere Langlebigkeit und bestenfalls auch bessere Energieabsorption als normale Eisen aufweisen.

8. References

Bowker, R. M., & Linder, K. E. (n.d.). Functional anatomy of the cartilage of the distal phalanx and digital cushion in the equine foot and a hemodynamic flow hypothesis of energy dissipation. 9.

Brommundt, E., Sachs, G., & Sachau, D. (2007). Technische Mechanik: Eine Einführung (4., verb. und erw. Aufl). Oldenbourg.

Cheramie, H. S., & O'Grady, S. E. (2003). Hoof repair and glue-on shoe adhesive technology. Veterinary Clinics of North America: Equine Practice, 19(2), 519–530. https://doi.org/10.1016/S0749-0739(03)00021-X

Daradka, M., & Pollitt, C. C. (n.d.). Epidermal cell proliferation in the equine hoof wall. 6.

Halsberghe, B. T. (2018). Effect of two months whole body vibration on hoof growth rate in the horse: A pilot study. Research in Veterinary Science, 119, 37–42. https://doi.org/10.1016/j.rvsc.2018.05.010

Hamel, G. (1912). Elementare Mechanik. B.G. Teubner. https://books.google.de/books?id=mvgNAwAAQBAJ

Horan, K., Kourdache, K., Coburn, J., Day, P., Carnall, H., Harborne, D., Brinkley, L., Hammond, L., Millard, S., Lancaster, B., & Pfau, T. (2021). The effect of horseshoes and surfaces on horse and jockey centre of mass displacements at gallop. PLOS ONE, 16(11), e0257820. https://doi.org/10.1371/journal.pone.0257820

Imhof, U. (2004). Die Chronologie der Hufeisen aus Schweizer Fundstellen. Schweizer Archiv für Tierheilkunde, 146(1), 17–25. https://doi.org/10.1024/0036-7281.146.1.17

Kasapi, M. A., & Gosline, J. M. (n.d.). DESIGN COMPLEXITY AND FRACTURE CONTROL IN THE EQUINE HOOF WALL. 21.

McKittrick, J., Chen, P.-Y., Bodde, S. G., Yang, W., Novitskaya, E. E., & Meyers, M. A. (2012). The Structure, Functions, and Mechanical Properties of Keratin. JOM, 64(4), 449–468. https://doi.org/10.1007/s11837-012-0302-8

Medina-Torres, C. E., Underwood, C., Pollitt, C. C., Castro-Olivera, E. M., Hodson, M. P., Richardson, D. W., & van Eps, A. W. (2016). The effect of weightbearing and limb load cycling on equine lamellar perfusion and energy metabolism measured using tissue microdialysis: Effects of weightbearing and limb cycling on lamellar physiology. Equine Veterinary Journal, 48(1), 114–119. https://doi.org/10.1111/evj.12377

Mishra, P. C., & Leach, D. H. (1983). Extrinsic and intrinsic veins of the equine hoof wall. Journal of Anatomy, 136(Pt 3), 543–560.

O'Grady, S. E., & Poupard, D. A. (2003). Proper physiologic horseshoeing. Veterinary Clinics of North America: Equine Practice, 19(2), 333–351. https://doi.org/10.1016/S0749-0739(03)00020-8

Parks, A. (2003). Form and function of the equine digit. Veterinary Clinics of North America: Equine Practice, 19(2), 285–307. https://doi.org/10.1016/S0749-0739(03)00018-X

Peham, C.& Schramel, J. (2017). METHOD AND DEVICE FOR DETERMINING THE COEFFICIENT OF FRICTION BETWEEN THE SURFACE OF A TEST OBJECT, IN PARTICULAR OF A BASE AND THE SURFACE OF A TEST BODY (Patent Nr. EP3141886 (A1)). Europäisches Patentamt. https://worldwide.espacenet.com/publicationDetails/biblio?locale=en_EP&date=20170315&CC=EP&NR=3141886A1&ND=4&KC=A1&rnd=1669923434684&FT=D&DB=

Pollitt, C. C. (1996). Basement membrane pathology: A feature of acute equine laminitis. Equine Veterinary Journal, 28(1), 38–46. https://doi.org/10.1111/j.2042-3306.1996.tb01588.x

Pollitt, C. C. (2004). Anatomy and physiology of the inner hoof wall. Clinical Techniques in Equine Practice, 3(1), 3–21. https://doi.org/10.1053/j.ctep.2004.07.001

Pollitt, C. C. (2010). The Anatomy and Physiology of the Suspensory Apparatus of the Distal Phalanx. Veterinary Clinics of North America: Equine Practice, 26(1), 29–49. https://doi.org/10.1016/j.cveq.2010.01.005

Roth, S., & Stahl, A. (2016). Reibung. In S. Roth & A. Stahl, Mechanik und Wärmelehre (pp. 145–157). Springer Berlin Heidelberg. https://doi.org/10.1007/978-3-662-45304-9_9

Schumacher, J., Schramme, M. C., Schumacher, J., & DeGraves, F. J. (2013). Diagnostic analgesia of the equine digit: Diagnostic analgesia of the equine digit. Equine Veterinary Education, 25(8), 408–421. https://doi.org/10.1111/eve.12001

Schummer, A., & Nickel, R. (1981). The Circulatory System, the Skin, and the Cutaneous Organs of the Domestic Mammals. P. Parey. https://books.google.at/books?id=uQ6TjwEACAAJ

Tan, H., & Wilson, A. M. (2011). Grip and limb force limits to turning performance in competition horses. Proceedings of the Royal Society B: Biological Sciences, 278(1715), 2105–2111. https://doi.org/10.1098/rspb.2010.2395

Vetmeduni. (2015). Vetmeduni Vienna: The Grip - Vienna Equine Surface Grip Test [Video]. YouTube. https://www.youtube.com/watch?v=IvbQJomkL_8

9. Appendix

Nr. of measurement	Dry concrete	Wet concrete	Dry asphalt	Wet asphalt	Gras	Sand	Ice
1	9.1	12.5	10.9	13.3	19.6	9	11.1
2	6.9	6	5.8	10.4	16.6	7.1	8.2
3	12.9	13.4	8.8	13.2	10.8	8	6.1
4	13.8	17.6	21.4	15.9	11.5	7.7	5.2
5	23.8	23.2	8	10.4	6.9	7.1	6.2
6	12.8	18.5	9.6	7.7	13.2	9.8	5.2
7	15.9	11.3	10.7	13	11.1	5.5	5.2
8	12.8	13.9	9.3	7.2	16.6	8.2	9.9
9	18.5	9	9.5	12	18.3	8.2	5.1
10	23	18.3	5.3	8.8	16.6	7.5	5.4
11	10.9	19.3	12.7	13	18.1	7	5.5
12	13.8	17.4	10.4	8.7	18.8	7.7	6.1
13	10.6	11.8	9.2	8	18.9	6.6	6.6
14	20.8	26.2	14.2	10.6	17.9	6.6	5.7
15	13.2	15.9	9.3	10.4	23.1	10.1	5.8
16	16.6	6	16.8	12.4	16.2	7.9	5.3
17	7.6	15.8	7.1	10.8	16.8	7.6	6.7
18	11	10.2	10.6	10.4	19.6	8.3	7.3
19	8.8	13.1	7.8	9.8	19.3	7.8	7.6
20	15.3	11.6	12.6	6.8	19.2	7.9	5.8
Average	13.90	14.55	10.5	10.64	16.46	7.78	6.5
Standard Dev.	4.77	5.20	3.74	2.38	3.88	1.06	1.63

Table 3: individual measurements of the iron shoe on all surfaces in Nm including the average value and standard deviation

Nr. of measurement	Dry concrete	Wet concrete	Dry asphalt	Wet asphalt	Gras	Sand	Ice
1	13	25.6	15.2	26.1	24.2	5.8	6.5
2	27	14.5	27.7	19.5	26.1	6.7	11.5
3	32.7	8.6	15.9	26.1	23.4	5.8	11.6
4	27.9	18.6	25.7	14.6	22	6.6	16.2
5	17.7	18.8	10.7	30.9	19.6	6.6	8.7
6	19.9	13.5	17.1	17.8	26.6	7.8	8.1
7	33.3	14.9	16.4	19.6	26.7	7	15
8	11.7	19.4	10.2	17.7	22.1	6.3	6.5
9	35.4	11.4	19.7	16	25.9	8.3	8.3
10	20.5	7.9	29.8	24.9	26	7.6	8.3
11	26.5	13.1	27.5	29.6	23.4	6.3	18
12	29.6	12.9	30.4	11.7	12.2	7	7.3
13	17.4	24.2	16.5	21.9	14.7	8.1	10.6
14	32.2	16.4	17.1	27.4	27.6	6.9	7.9
15	10.2	13.9	19.4	10.8	31.	5.5	12.1
16	18.8	12.6	16	23.5	22.8	8	12.3
17	28.8	28.2	27.1	13.3	26.8	7.3	7.8
18	12.8	19.8	10.3	10.2	19.2	5.3	13.4
19	27.5	21.2	15.7	26.9	23.8	7	6.3
20	9	30.6	20.7	25	27	7.3	8.2
Average	22.60	17.31	19.46	20.68	23.56	6.86	10.23
Standard Dev.	8.49	6.24	6.45	6.46	4.47	0.86	3.42

Table 4: individual measurements of the natural bare hoof on all surfaces in Nm including the average value and standard deviation

Nr. of measurement	Dry concrete	Wet concrete	Dry asphalt	Wet asphalt	Gras	Sand	Ice
1	16.4	20.1	13.5	22.1	23.8	8.7	8
2	18.3	19.1	20.6	23.6	21.2	10.9	24.9
3	18	26	20.3	30.8	21.6	8.1	9.4
4	21.4	27.3	17	21.9	23.5	9	8.9
5	18.8	18.6	11.8	26.3	22.9	10.4	8
6	22.4	28.8	17.4	16.3	26.4	7.1	17.8
7	23.2	25.9	14.2	27.9	27.8	7.2	17.9
8	29	18.1	26.2	22.2	23.7	10.9	7.8
9	27.3	18.6	14.7	25.2	22.6	5.8	14.6
10	20.3	19.2	20.6	20.6	22.5	9.5	7.5
11	27	16.3	24.1	23.1	22.1	7.9	20.3
12	22.7	21.7	23.8	23.8	23.6	9.7	8.1
13	34.2	18.6	27.6	19.9	20	8.9	10.4
14	23.8	21.4	27.3	13.1	24.1	10.7	6.6
15	20.6	17.8	17.8	24.7	22.4	9.9	13.7
16	25.1	16.6	19	25.1	27.9	9.1	23.7
17	18.5	21	18.8	19.5	21.6	9.6	16.6
18	17.1	25.8	28.4	34.9	20.8	9.7	12.5
19	17.5	20.2	24.4	25.8	21.9	10	8.7
20	21.7	26.4	19.4	24.1	22.7	5.5	10.6
Average	22.17	21.38	20.35	23.55	23.16	8.9	12.8
Standard Dev.	4.58	3.87	4.94	4.74	2.12	1.57	5.64

Table 5: individual measurements of the grip plate application on all surfaces in Nm including the average value and standard deviation

Nr. of measurement	Dry concrete	Wet concrete	Dry asphalt	Wet asphalt	Gras	Sand	Ice
1	28.7	13.9	17.6	20.1	25.1	9.4	6.9
2	33.4	19.6	20.7	16.9	22	10.2	6.6
3	17.2	23.1	16.3	23.4	19.8	10.3	5.2
4	22	23	27.9	20.7	22.1	10.6	8.8
5	28.8	28.8	23.8	22	18.1	10.8	6.6
6	32.9	31.1	14.3	17.5	19.3	10.3	7.3
7	26.1	22.9	21.5	17.9	20.8	9.8	14.5
8	25.8	31.4	32.8	16.3	24.1	8.8	12
9	17.8	20	16.3	18.3	24.4	8.7	18.3
10	17.4	17.6	25.3	19.6	22.2	10.6	8.1
11	21.1	23.8	15.4	23.6	17.7	10.2	7.2
12	6.7	15.2	28.3	20	24.6	8.1	10.6
13	29.4	25.9	31.7	15.8	21.4	7.2	5.3
14	19.4	22.3	24.2	17.6	22.2	7.9	8.4
15	27.9	30.1	26.4	8.7	22.9	10.8	9.2
16	26.7	32.7	22.3	27.3	22.2	5.4	5.2
17	22.3	21.4	15.7	19.1	21.5	5.8	6.7
18	30.2	18.7	18.2	19.9	17.6	8.4	9.4
19	26.1	25.6	22.8	21.6	19.6	5.4	8.6
20	18.9	17.9	26.7	19.8	20.3	8.8	5.8
Average	23.94	23.25	22.41	19.31	21.40	8.88	8.54
Standard Dev.	6.50	5.48	5.56	3.73	2.25	1.78	3.29

Table 6: individual measurements of the artificial bare hoof on all surfaces in Nm including the average value and standard deviation